

# Pronounced energy absorption capacity of cellular bulk metallic glasses

Cite as: Appl. Phys. Lett. **104**, 111907 (2014); <https://doi.org/10.1063/1.4869229>

Submitted: 18 February 2014 . Accepted: 11 March 2014 . Published Online: 19 March 2014

S. H. Chen, K. C. Chan, F. F. Wu, and L. Xia



View Online



Export Citation



CrossMark

## ARTICLES YOU MAY BE INTERESTED IN

[Enhancement of room-temperature plasticity in a bulk metallic glass by finely dispersed porosity](#)

Applied Physics Letters **86**, 251907 (2005); <https://doi.org/10.1063/1.1953884>

[Syntactic bulk metallic glass foam](#)

Applied Physics Letters **84**, 1108 (2004); <https://doi.org/10.1063/1.1646467>

[Amorphous metallic foam](#)

Applied Physics Letters **82**, 370 (2003); <https://doi.org/10.1063/1.1537514>

Lock-in Amplifiers  
up to 600 MHz



# Pronounced energy absorption capacity of cellular bulk metallic glasses

S. H. Chen,<sup>1</sup> K. C. Chan,<sup>1,a)</sup> F. F. Wu,<sup>1,2</sup> and L. Xia<sup>1</sup>

<sup>1</sup>Advanced Manufacturing Technology Research Centre, Department of Industrial and Systems Engineering, The Hong Kong Polytechnic University, Hung Hom, Kowloon, Hong Kong

<sup>2</sup>School of Materials Science and Engineering, Liaoning University of Technology, Jinzhou 121001, China

(Received 18 February 2014; accepted 11 March 2014; published online 19 March 2014)

Cellular bulk metallic glasses (BMGs) with macroscopic cellular structures were designed and fabricated. The cellular BMGs exhibited remarkable energy absorption capacity as compared with reported BMG foams and honeycombs. The enhanced energy absorption capability is attributed to the large plastic bending of the struts, the blunting of the cracks, and the large plastic deformation at the nodes. This work shows that, in cellular BMGs, the macroscopic cellular structures are more efficient in dissipating mechanical energy than microscopic cellular structures, opening a window for developing energy absorption devices using BMGs. © 2014 AIP Publishing LLC.

<http://dx.doi.org/10.1063/1.4869229>

The dissipation of mechanical energy is vital in a wide range of applications such as the structural function of bones and nacles,<sup>1,2</sup> vehicle safety,<sup>3</sup> and the dynamic failure of cracks.<sup>4</sup> To increase the energy dissipation before a catastrophic failure, it requires both high strength and high toughness of the particular material. However, there is a well-known contradiction between these two factors in that an increase in strength will cause a decrease in toughness.<sup>5</sup> Thus, how to increase the energy dissipation becomes a crucial issue. Research on human bones shows that the breaking of the fibril arrays and the crack bridging of collagen fibrils and ligaments behind a crack tip can increase the energy dissipation to stop the cracks from growing.<sup>6,7</sup> The enlargement of the plastic deformation zone ahead of the crack tip can also dissipate more energy to shield against the activation of cracks.<sup>8</sup> The introduction of microscopic pores into metals has enabled a high efficiency in dissipating mechanical energy to be achieved through the formation of a wide plateau of irreversible plastic flow.<sup>3</sup> In addition to high energy absorption capacity, cellular metals also have large strength to weight ratios, which are extremely useful in developing devices for energy absorption purposes and for light-weight constructions.<sup>9</sup>

Recently, building on a new class of metals, bulk metallic glasses (BMGs), which have relatively larger strength than their crystalline counterparts, BMG foams<sup>10–13</sup> and honeycombs<sup>14,15</sup> have been developed, exhibiting greatly enhanced energy absorption capability as compared with the commercial cellular metals, such as Al foams. However, the microstructure of BMG foams is difficult to control accurately, and the fabrication of BMG honeycombs is limited to 2D structures, which significantly hinder their applications. In this Letter, we report a kind of 3D cellular BMG, constructed with a macroscopic cellular structure, which demonstrates remarkable efficiency in dissipating mechanical energy under compression testing.

As-cast Zr<sub>57</sub>Cu<sub>20</sub>Al<sub>10</sub>Ni<sub>8</sub>Ti<sub>5</sub> (at. %) BMG rods, 5 mm in diameter, were produced by copper mold suction casting.<sup>16</sup>

The amorphous state of the as-cast specimens was confirmed using standard X-ray diffraction (XRD) analysis on a Rigaku SmartLab X-ray diffractometer. The glass transition temperature ( $T_g$ ) of the BMGs was determined as 665 K using differential scanning calorimetry (DSC) analysis on a Perkin-Elmer DSC7 machine at a heating rate of 40 K/min. The compressive stress-strain deformation behavior of the as-cast rods and the XRD patterns as well as the DSC curves is shown in Figure 1. The 3D cellular BMGs were fabricated from the as-cast rods according to the schematic diagram shown in Figure 2, using wire-cut electrical discharge machining (EDM) on an FI 240 SLP wire-cut EDM machine. Three specimens with  $l=1.2$  mm, 1.0 mm, and 0.8 mm (where  $l$  is the width of the strut) were prepared as shown in Fig. 2, with relative densities calculated as 0.67, 0.59, and 0.49, respectively. The relative densities of the cellular BMGs were determined from the expression

$$\rho_r = \frac{\rho_c}{\rho_s} = \frac{2\sqrt{2}l}{H} - \frac{2l^2}{H^2}, \quad (1)$$

where  $\rho_c$  and  $\rho_s$  are the densities of the cellular BMGs and the as-cast BMGs, respectively. The compressive deformation behavior of the cellular BMGs was tested on a

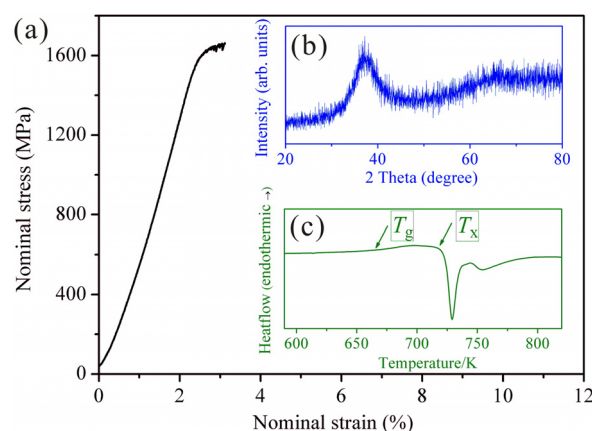


FIG. 1. (a) Compressive deformation behavior of 5 mm as-cast rods. (b) and (c) The XRD pattern and DSC curve of the specimen, respectively.

<sup>a)</sup> Author to whom correspondence should be addressed. Electronic mail: [kc.chan@polyu.edu.hk](mailto:kc.chan@polyu.edu.hk). Tel.: 852-2766-4981.

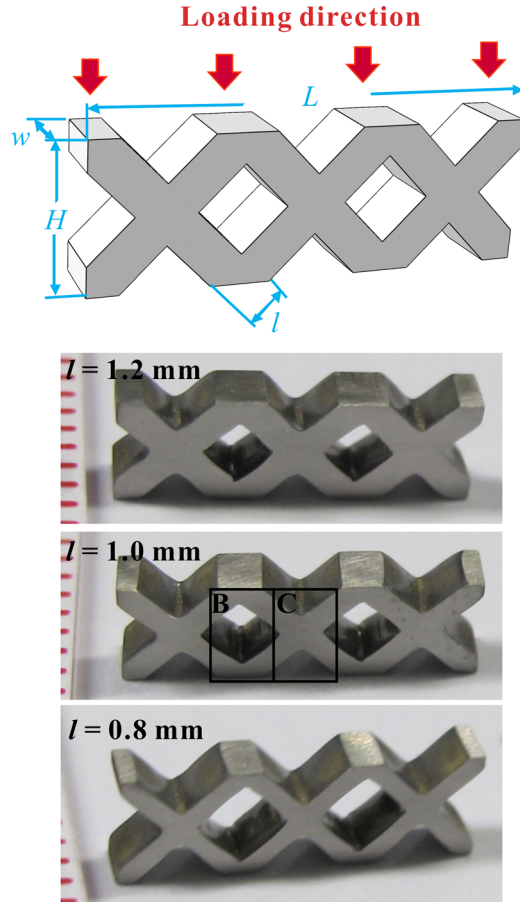


FIG. 2. Schematic diagram of the cellular BMGs, where  $H=3.96$  mm,  $w=2.0$  mm,  $L=11.88$  mm, and  $l=1.2$  mm,  $1.0$  mm, and  $0.8$  mm, and the optical images of the prepared specimens.

servo-hydraulic 810 Materials Testing System with a constant cross-head loading speed of  $0.024$  mm/min. After densification, the side surfaces of the specimens were examined using a Jeol JSM-6490 scanning electron microscope (SEM).

Figure 3(a) shows the nominal stress vs. macroscopic strain curves of the cellular BMGs. Compared with the stress-strain behavior of as-cast BMGs (Fig. 1(a)), the cellular BMGs have much larger macroscopic strains. The macroscopic strain of the cellular BMGs involves three stages: the elastic stage, the plastic-flow plateau stage, and the densification stage. After reaching the peak stress, the specimen with  $\rho_r=0.67$  fractured at a nominal strain of about 14%, while the specimens with  $\rho_r=0.59$  and  $0.49$  have much larger plastic-flow plateaus till densification of the cellular structures occurs.

To characterize the mechanical energy dissipation during the compression of the cellular BMGs, the energy absorption per unit volume ( $W_v$ ) is calculated according to the equation<sup>17</sup>

$$W_v = \int_0^{\varepsilon_D} \sigma(\varepsilon) d\varepsilon, \quad (2)$$

where  $\sigma(\varepsilon)$  is the nominal stress and  $\varepsilon_D$  the macroscopic strain. The energy absorption capacity vs. the macroscopic

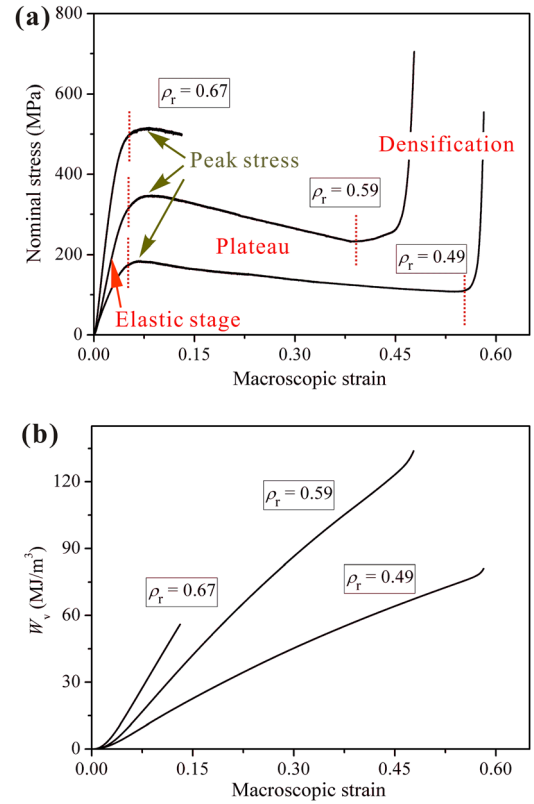


FIG. 3. (a) The compressive responses of the cellular BMGs and (b) the evolution of the energy absorption capacity of the cellular BMGs.

strain curves are shown in Fig. 3(b). The maximum  $W_v$  value occurs in the cellular BMG with  $\rho_r=0.59$ , which suggests that this cellular BMG has higher energy absorption capability.

Figure 4(a) shows the comparison of the energy absorption capacity of the present cellular BMGs and the reported BMG foams<sup>10–12,18</sup> and honeycombs,<sup>15</sup> with various relative densities. The energy absorption capacity of the as-cast BMG with 5 mm in diameter is also shown here for comparison. It can be seen that the cellular BMG with  $\rho_r=0.59$  has the largest energy absorption capacity. When the  $\rho_r$  increases to 0.67, the limited macroscopic plastic strain (Fig. 3(a)) results in relatively lower energy absorption capacity. When the  $\rho_r$  decreases to 0.49, although the plastic-flow plateau is increased to about 0.5 (Fig. 3(a)), a lower nominal stress causes the energy absorption capacity to decrease (Fig. 3(b)). Nevertheless, the cellular BMGs are much better than the reported BMG foams and honeycombs. For example, even the cellular BMG ( $\rho_r=0.67$ ) having catastrophic failure has a higher energy absorption capacity than that of the BMG foams with similar relative densities. Besides the enhanced energy absorption capacity, the cellular BMGs have a larger relative density (about 0.67) for ductile-to-brittle transition than the BMG honeycombs (0.4),<sup>15</sup> which can result in increased nominal stress and more energy dissipation. A previous study has found that the energy absorption capacity of cellular materials were mainly determined by two factors: the strength of the materials and the deformation behavior of the cellular structures.<sup>18</sup> In the case of metallic glass foams, the higher strength of the BMGs contributes to the improvement of the energy absorption capacity. In the present study,

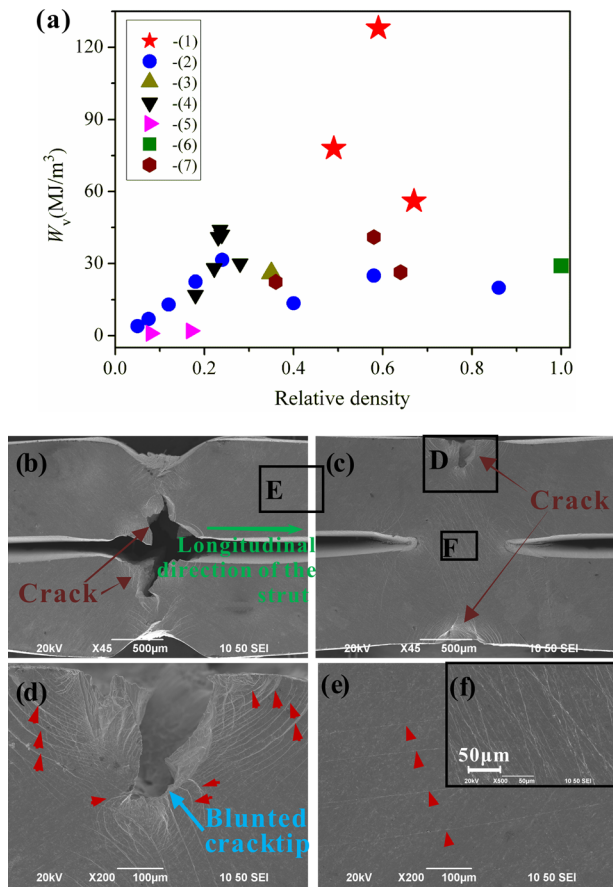


FIG. 4. (a) Comparison of the energy absorption per unit volume of some cellular BMG structures: (1) The  $Zr_{57}Cu_{20}Al_{10}Ni_8Ti_5$  BMG cellular structures in the present study; (2)  $Zr_{35}Ti_{30}Cu_{7.5}Be_{27.5}$  BMG honeycombs;<sup>15</sup> (3)  $Zr_{41.25}Ti_{13.75}Cu_{12.5}Ni_{10}Be_{22.5}$  BMG foam;<sup>18</sup> (4)  $Zr_{57}Cu_{15.4}Ni_{12.6}Al_{10}Nb_5$  BMG foam;<sup>12</sup> (5)  $Pd_{43}Cu_{27}P_{20}Ni_{10}$  BMG foam;<sup>11</sup> (6) solid  $Zr_{57}Cu_{20}Al_{10}Ni_8Ti_5$  BMG rods with 5 mm in diameter; (7)  $Pd_{42.5}Cu_{30}P_{20}Ni_{7.5}$  BMG foam.<sup>10</sup> (b)-(f) Magnified SEM micrographs of the rectangles (B) and (C) in Fig. 2 and (D)-(F) in Figs. 4(b) and 4(c) correspondingly. Arrows in (d) and (e) indicate the formation of shear bands.

the  $ZrCuNiAlTi$  BMG that was chosen for the cellular BMGs does not show prominent mechanical properties, i.e., the yield strength of this BMG is smaller than some other BMGs (see Table I). However, the cellular  $ZrCuNiAlTi$  BMG shows pronounced energy absorption capacity as compared with other BMG foams and honeycombs. Therefore, the well designed macroscopic cellular structure is the main factor resulting in these excellent properties.

By further investigating the mechanism at the micro-scale, the energy dissipation in cellular BMGs can be evidenced by the formation shear bands. After densification, the

side surfaces of the cellular BMG with  $\rho_r = 0.59$  are shown in the SEM images in Figs. 4(b)–4(f). First, at the ends of the struts, a large number of shear bands can be found, as in Figs. 4(b) and 4(c), implying that a large amount of the energy has been dissipated.<sup>22</sup> Moreover, the formation of profuse shear bands around the cracks (Fig. 4(d)) further increase the energy dissipation before catastrophic failure of the cracks.<sup>8</sup> Second, differing from conventional bending tests where the neutral planes have no stress, some shear bands nearly parallel to the longitudinal direction of the struts have been observed in the middle of the struts (Figs. 4(b) and 4(e)). This phenomenon reveals that some plastic shearing flow occurs in the middle of the struts, in the longitudinal direction of the struts, which definitely results in an increase in the amount of energy being dissipated. Third, large plastic deformation occurs at the nodes of the cellular BMGs (Fig. 4(c)). As shown in the magnified micrograph in Fig. 4(f), the formation of dense shear bands and the intersection of the shear bands can also dissipate a large amount of energy during the loading process.<sup>23</sup>

It should be pointed out that, in contrast to the BMG foams and honeycombs where buckling plays an important role in dissipating energy, buckling of the struts is rarely found in cellular BMGs. According to Euler's buckling theory, the critical load for the buckling of a both ends fixed strut in a cellular BMG can be calculated using the equation,<sup>24</sup>

$$P_c = \frac{4\pi^2 EI}{b^2}, \quad (3)$$

where  $E$  is the Young's modulus of the solid BMG,  $I = wl^3/12$  is the second moment area of the cross section of the strut, and  $b$  the length of the strut. For simplicity, if we assume that the angle of the strut is still maintained at about  $45^\circ$  when buckling occurs, the critical buckling load for the strut along the loading direction can be estimated as  $\sqrt{2} P_c$ . The critical load components ( $\sqrt{2} P_c$ ) for a both ends fixed strut in the three cellular BMGs with  $\rho_r = 0.67$ ,  $0.59$ , and  $0.49$  were calculated as 168 kN, 97 kN, and 50 kN, respectively, which are much larger than the peak loads of the whole cellular BMG structures (about 12 kN, 8 kN, and 4 kN, respectively), implying that the buckling of struts in these cellular BMGs is not likely to occur. Therefore, the buckling effect in the present cellular BMG specimens is negligible.

The pronounced energy absorption capacity of cellular BMGs highly depends on the bending behavior of BMGs. Since Zr-based BMGs with thicknesses no larger than 1 mm have large bending plasticity,<sup>25</sup> hence the strut thickness ( $l$ ) in the design of cellular BMGs is critical. When  $l$  increases to 1.2 mm, the specimen exhibits catastrophic failure at a plastic strain of about 10%. The relatively poor plastic deformation behavior lessens the amount of energy being dissipated. When the strut thickness decreases from 1 mm to 0.8 mm, the peak stress of the cellular structure decreases from 356 MPa to 184 MPa (as indicated in Fig. 3). This also decreases the energy absorption capacity. Since the energy dissipation through the bending of the struts plays a significant role in BMG foams<sup>12,18</sup> and honeycombs,<sup>15</sup> the small cross-sectional dimension of the struts in BMG foams and honeycombs leads to smaller peak stress, and subsequently a

TABLE I. The yield strength of the parent BMGs for the cellular BMG structures.

Parent BMGs	Yield strength/GPa	Ref.
$Zr_{57}Cu_{20}Al_{10}Ni_8Ti_5$	1.635	Present work
$Zr_{35}Ti_{30}Cu_{7.5}Be_{27.5}$	1.43	19
$Zr_{41.25}Ti_{13.75}Cu_{12.5}Ni_{10}Be_{22.5}$	1.9	20
$Zr_{57}Cu_{15.4}Ni_{12.6}Al_{10}Nb_5$	1.75	21
$Pd_{43}Cu_{27}P_{20}Ni_{10}$	1.63	11
$Pd_{42.5}Cu_{30}P_{20}Ni_{7.5}$	1.65	10



smaller energy absorption capability. This could be a critical reason for the enhancement of the energy absorption capacity of cellular BMGs compared with BMG foams and honeycombs. On the other hand, as compared with the energy dissipation processes through the buckling, plastic bending and the collapse of the struts in BMG foams<sup>12,18</sup> and honeycombs,<sup>15</sup> strut collapse does not occur in cellular BMGs with  $\rho_r = 0.49$  and  $0.59$ . The energy dissipation is achieved through the plastic bending of the struts, including the formation of cracks, and the large plastic deformation at the nodes. The change of the energy dissipation mechanisms implies that more energy is dissipated through the localized plastic shearing process in cellular BMGs.

The large plastic-flow plateaus (Fig. 3(a)) indicate that the blunting of the crack tips or shear banding prohibition approaches to avoid catastrophic failure. A plastic zone in the front of the crack tip has an important role influencing the blunting of a crack.<sup>5,8</sup> A large plastic zone means a higher toughness. The radius of the plastic zone ahead of the crack tip in the present BMGs can be estimated from the equation,<sup>8</sup>

$$r_p = \frac{K_c^2}{\pi \sigma_y^2}. \quad (4)$$

By taking the fracture toughness of  $K_c$  as  $69 \text{ MPa m}^{1/2}$ ,<sup>26</sup> the radius of the plastic zone is estimated as  $0.6 \text{ mm}$ . This value is critical in blunting the crack to achieve large energy dissipation in cellular BMGs, where the struts have thicknesses no larger than  $1 \text{ mm}$ . Crack blunting can be verified by observation of the circular shear bands around the cracks, as indicated by the arrows in Fig. 4(d). The cavitation event (the shear flow capacity before cavitation) for initiating a crack in the present BMGs can be scaled by a dimensionless parameter  $f$ <sup>8</sup>

$$\log(f) \sim \frac{W_s}{k_B T} \left( \frac{W_c}{W_s} - 1 \right) \sim \frac{T_g}{T} \left( \frac{B}{G} - 1 \right), \quad (5)$$

where the bulk modulus  $B$  and shear modulus  $G$  are  $99.2 \text{ GPa}$  and  $30.1 \text{ GPa}$ , respectively,<sup>27</sup> and  $T$  is taken as  $300 \text{ K}$ .<sup>8</sup> The magnitude of  $\log(f)$  is estimated at  $5.1$ , which is larger than the values of Mg-based BMGs ( $1.9$ ) and La-based BMGs ( $2.6$ ) with much smaller plastic zone radii of less than  $30 \mu\text{m}$ .<sup>8</sup> This indicates that the high blunting effect of the crack tips in this BMG can be attributed to the large difference between the activation barriers for shearing flow ( $W_s$ ) and cavitation ( $W_c$ ).<sup>8</sup>

To achieve a higher energy absorption capacity in cellular metals, many research studies have focused on tailoring microscopic cellular structures in BMGs, such as closed cell foams,<sup>10,28–30</sup> open-cell foams,<sup>12,13,31,32</sup> pore sizes,<sup>12,33</sup> honeycomb structures,<sup>14,15</sup> and the thickness of the ligaments.<sup>15</sup> In the present cellular BMGs, the large plastic deformation in both the struts and nodes demonstrates a higher efficiency in dissipating the mechanical energy. As compared with other BMGs, the  $r_p$  and  $\log(f)$  values of the present BMG are representative of Zr-based BMGs,<sup>8</sup> which suggests that the high energy absorption capacity of the macroscopic cellular structures in the present work could also be suitable for other Zr-based BMGs. This work opens up a window for the design of cellular metals using BMGs in order to achieve

larger energy absorption capability: not by tuning the buckling and bending of the struts through microscopic cellular changes, but to obtain optimum macroscopic bending of the struts and large plastic deformation at the nodes through constructing macroscopic cellular structures.

In summary, a type of cellular BMGs has been designed, which demonstrates a larger energy absorption capability when compared with BMG foams and honeycombs. The results show that the energy dissipation in cellular BMGs through the large plastic deformation of the struts and nodes has better efficiency than the buckling, bending, and collapse of struts in BMG foams and honeycombs. This research provides guidance in designing cellular BMG structures for energy absorption applications.

This work was fully funded by the Research Committee of the Hong Kong Polytechnic University under research student project account code RPTD.

- <sup>1</sup>H. Peterlik, P. Roschger, K. Klaushofer, and P. Fratzl, *Nature Mater.* **5**, 52 (2006).
- <sup>2</sup>Z. Y. Tang, N. A. Kotov, S. Magonov, and B. Ozturk, *Nature Mater.* **2**, 413 (2003).
- <sup>3</sup>J. Banhart, *Prog. Mater. Sci.* **46**, 559 (2001).
- <sup>4</sup>E. Sharon, S. P. Gross, and J. Fineberg, *Phys. Rev. Lett.* **76**, 2117 (1996).
- <sup>5</sup>R. O. Ritchie, *Nature Mater.* **10**, 817 (2011).
- <sup>6</sup>R. K. Nalla, J. H. Kinney, and R. O. Ritchie, *Nature Mater.* **2**, 164 (2003).
- <sup>7</sup>K. J. Koester, J. W. Ager, and R. O. Ritchie, *Nature Mater.* **7**, 672 (2008).
- <sup>8</sup>M. D. Demetriou, M. E. Launey, G. Garrett, J. P. Schramm, D. C. Hofmann, W. L. Johnson, and R. O. Ritchie, *Nature Mater.* **10**, 123 (2011).
- <sup>9</sup>A. G. Evans, J. W. Hutchinson, and M. F. Ashby, *Prog. Mater. Sci.* **43**, 171 (1998).
- <sup>10</sup>T. Wada and A. Inoue, *Mater. Trans.* **45**, 2761 (2004).
- <sup>11</sup>M. D. Demetriou, C. Veazey, J. S. Harmon, J. P. Schramm, and W. L. Johnson, *Phys. Rev. Lett.* **101**, 145702 (2008).
- <sup>12</sup>A. H. Brothers and D. C. Dunand, *Acta Mater.* **53**, 4427 (2005).
- <sup>13</sup>A. H. Brothers and D. C. Dunand, *Adv. Mater.* **17**, 484 (2005).
- <sup>14</sup>B. Sarac, J. Ketkaew, D. O. Popnoe, and J. Schroers, *Adv. Funct. Mater.* **22**, 3161 (2012).
- <sup>15</sup>B. Sarac and J. Schroers, *Scr. Mater.* **68**, 921 (2013).
- <sup>16</sup>S. H. Chen, K. C. Chan, and L. Xia, *Mater. Sci. Eng., A* **574**, 262 (2013).
- <sup>17</sup>L. J. Gibson and M. F. Ashby, *Cellular Solids Structure and Properties* (Cambridge University Press, Cambridge, 1997), p. 314.
- <sup>18</sup>X. Wei, J. H. Chen, and L. H. Dai, *Scr. Mater.* **66**, 721 (2012).
- <sup>19</sup>G. Duan, A. Wiest, M. L. Lind, J. Li, W. K. Rhim, and W. L. Johnson, *Adv. Mater.* **19**, 4272 (2007).
- <sup>20</sup>R. D. Conner, R. B. Dandliker, and W. L. Johnson, *Acta Mater.* **46**, 6089 (1998).
- <sup>21</sup>H. Choi-Yim, R. Busch, U. Koster, and W. L. Johnson, *Acta Mater.* **47**, 2455 (1999).
- <sup>22</sup>W. J. Wright, T. C. Hufnagel, and W. D. Nix, *J. Appl. Phys.* **93**, 1432 (2003).
- <sup>23</sup>B. A. Sun and W. H. Wang, *Appl. Phys. Lett.* **98**, 201902 (2011).
- <sup>24</sup>R. Subramanian, *Strength of materials* (Oxford University Press, New Delhi, 2010), p. 656.
- <sup>25</sup>R. D. Conner, Y. Li, W. D. Nix, and W. L. Johnson, *Acta Mater.* **52**, 2429 (2004).
- <sup>26</sup>J. H. Schneibel, J. A. Horton, and P. R. Munroe, *Metall. Mater. Trans. A* **32**, 2819 (2001).
- <sup>27</sup>W. H. Wang, R. J. Wang, G. J. Fan, and J. Eckert, *Mater. Trans.* **42**, 587 (2001).
- <sup>28</sup>J. Schroers, C. Veazey, and W. L. Johnson, *Appl. Phys. Lett.* **82**, 370 (2003).
- <sup>29</sup>A. H. Brothers and D. C. Dunand, *Appl. Phys. Lett.* **84**, 1108 (2004).
- <sup>30</sup>T. Wada, A. Inoue, and A. L. Greer, *Appl. Phys. Lett.* **86**, 251907 (2005).
- <sup>31</sup>A. H. Brothers, R. Scheunemann, J. D. DeFouw, and D. C. Dunand, *Scr. Mater.* **52**, 335 (2005).
- <sup>32</sup>T. Wada and A. Inoue, *Mater. Trans.* **44**, 2228 (2003).
- <sup>33</sup>T. Wada, K. Takenaka, N. Nishiyama, and A. Inoue, *Mater. Trans.* **46**, 2777 (2005).